Reversible Covalent Chemistry of CO_2: An Opportunity for Nano-Structured Hybrid Organic–Inorganic Materials

Johan Alauzun,[†] Eric Besson,[‡] Ahmad Mehdi,*[,†] Catherine Reyé,[†] and Robert J. P. Corriu*[,†]

Institut Charles Gerhardt Montpellier, UMR 5253 CNRS, Chimie moléculaire et organisation du solide, Université Montpellier II, Place E. Bataillon CC 1701, 34095 Montpellier, France, and Institut de Chimie Séparative de Marcoule UMR 5257 ICSM, Site de Marcoule BP 17171, 30207 Bagnols-sur-Cèze, France

Received July 20, 2007. Revised Manuscript Received October 3, 2007

A new approach to get ordered and highly amine-functionalized organosilicas is described. The method consisted of using the reversible reaction between CO_2 and amines giving rise to ammonium carbamate salts. Four amine containing precursors were selected for this study: 3-aminopropyltrimethoxysilane (**1**), 11-amino-undecyltrimethoxysilane (**2**), *N*-(2-aminoethyl)-3-aminopropyltrimethoxysilane (**3**), and *N*-(6-aminohexyl)-3-aminopropyltrimethoxysilane (**4**). CO_2 reacted with **1** and **2** affording bis-silylated organosilica precursors containing ammonium carbamate salts in the core while the reaction between CO_2 and **3** or **4** led to a supramolecular network of silylated ammonium carbamate salts. The hydrolytic polycondensation of these carbamate derivatives by using the sol–gel process provided hybrid materials with lamellar structure containing ammonium carbamate salts. Subsequent elimination of CO_2 upon heating generated materials with free amino groups in which the long-range order was maintained. The structuration was found to be highly dependent on van der Waals interactions between the long alkylene chains. Some complexation reactions and chemical transformations were achieved to investigate the accessibility of the amino groups as well as the chelating capability of the materials.

Introduction

Organically functionalized silicas obtained by the sol–gel process constitute a unique class of materials.[1] Indeed, by changing the nature of the organic moieties, it is possible to obtain materials presenting a large variety of properties with promising applications in many areas such as catalysis, separation, environment, optics, and so forth.[1] Among the different routes which could provide such materials, the use of bridged organosilica precursors with the general formula $[(R'O)_3Si]_mR$ ($m \geq 2$) is of special interest as they allow the formation of homogeneous hybrid organic–inorganic materials with generally a degree of local organization.[2] In spite of numerous studies concerning the structural organization of bridged silsesquioxanes, few examples of such materials with long-range order were reported.[3,4] Therefore, the control of the structure of hybrid materials during the sol–gel process remains a challenge and constitutes an exciting area of research in nanosciences and nanotechnology.

We have shown that it is possible to obtain long-range ordered bridged silsesquioxanes by playing only on the experimental conditions: While the hydrolytic polycondensation of α,ω-bis(trimethoxysilyl)alkylenes with long alkylene chains gives rise to amorphous solids in tetrahydrofuran (THF), in water there is formation of long-range ordered materials. The structuration was found to be highly dependent on the hydrophobic interactions between the long alkylene chains,[5] the length of the alkylene chains controlling the structure. These results prompted us to explore the formation of functional hybrid organic–inorganic materials from bridged organosilica precursors with long alkylene chains having a functionalized and chemically transformable core.

Thus, hydrolysis and polycondensation of α,ω-bis(trimethoxysilyl)alkyldisulfide in water provided lamellar bridged organosilica containing disulfide cores.[6] Subsequent reduction of disulfide cores gave rise to highly ordered organosilica with a high content of thiol groups. In that case, the functionalization of the materials was obtained by the cleavage of the covalent S−S bonds included within the hybrid materials. This study showed that it is possible to perform chemical transformations within an ordered material without a collapse of the structure.

As it is of great interest to find new routes to design functionalized and ordered materials, we decided to investigate the preparation of amino-functionalized materials by

* To whom correspondence should be addressed. E-mail: ahmad.mehdi@univ-montp2.fr (A.M.).
[†] Université Montpellier II.
[‡] Institut de Chimie Séparative de Marcoule.

(1) (a) Sanchez, C.; Julian, B.; Belleville, P.; Popall, M. *J. Mater. Chem.* **2005**, *15*, 3559.
(2) (a) Boury, B.; Corriu, R. J. P.; Le Strat, V.; Delord, P.; Nobili, M. *Angew. Chem., Int. Ed.* **1999**, *38*, 3172. (b) Boury, B.; Corriu, R. J. P. *Chem. Commun.* **2002**, 795. (c) Boury, B.; Corriu, R. J. P. *Chem. Rec.* **2003**, *3*, 120. (d) Lerouge, F.; Cerveau, G.; Corriu, R. J. P. *New J. Chem.* **2006**, *30*, 1364.
(3) Moreau, J. J. E.; Pichon, B.; Bied, C.; Wong Chi Man, M. *J. Mater. Chem.* **2005**, *15*, 3929.
(4) Liu, N.; Yu, K.; Smarsly, B.; Dunphy, D. R.; Jiang, Y. B.; Brinker, C. J. *J. Am. Chem. Soc.* **2002**, *124*, 14540.
(5) Alauzun, J.; Mehdi, A.; Reyé, C.; Corriu, R. J. P. *J. Mater. Chem.* **2005**, *15*, 841.
(6) Alauzun, J.; Mehdi, A.; Reyé, C.; Corriu, R. J. P. *Chem. Commun.* **2006**, 347.

10.1021/cm701946w CCC: $40.75
Published on Web 12/28/2007

Scheme 1

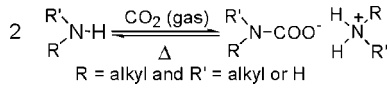

using CO_2 as an assembly agent.[7] Indeed, modified silicas containing amino groups are probably the most widely studied hybrid organic–inorganic materials. That is due to the numerous potential applications, which can proceed in particular as base catalyst or metal sorbents.[8,9] Amine containing materials were also often prepared in an effort to develop selective solid sorbents for gas removal, in particular CO_2.[10]

Actually, the reaction between CO_2 and a primary and secondary amine at ordinary temperature and pressure has been known for a long time.[11] The resulting ammonium carbamate salts are thermally unstable and release CO_2 upon heating (Scheme 1). Recently, this "old chemistry" has been successfully used.[12] Thus, reactions between CO_2 and immobilized amines have been employed for gas sensing.[13–15] Amine-containing ionic liquids were found trapping CO_2, which could be used in the purification of industrial gas mixtures.[16] Xu and Rudkevich used CO_2 gas to construct novel types of supramolecular polymers by employing both hydrogen bonds and dynamic thermally reversible carbamate bonds, which lead to switchable materials.[17]

In this contribution, we used the reversible covalent chemistry of CO_2 with amines. CO_2 acted as the bridging group to obtain at least a bis-silylated species allowing the formation of hybrid materials by hydrolytic polycondensation. Thermal treatment of the materials containing ammonium carbamate salts allowed the recovery of the free amino groups (Scheme 2).

Scheme 2

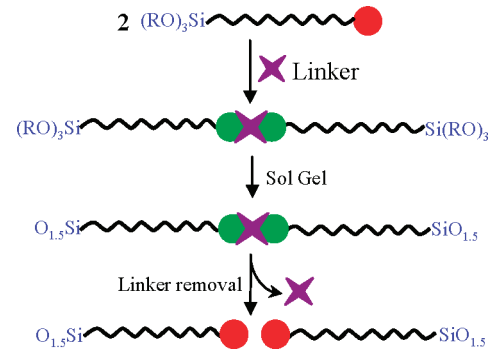

Scheme 3

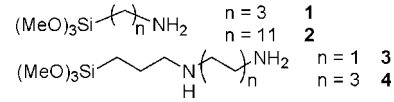

In the literature, there are several examples of bridged polysilsesquioxanes whose cleavage has been explored to bring chemical transformations. These include the use of the retro Diels–Alder reactions to modify[18] or cleave the bridging groups,[19] the decarboxylation of dialkylene carbonate-bridged polysilsesquioxane by thermal treatment giving new hydroxyalkyl and olefinic substituted polysilsesquioxane,[20] and the thermal decomposition of phenolic carbamate linkages.[19] More recently, the thermolysis of carbamate-bridged polysilsesquioxane was reported to obtain bulk silica containing isolated primary amines.[21]

Our approach involves the reaction between CO_2 and 3-aminopropyltrimethoxysilane (**1**), 11-amino-undecyltrimethoxysilane (**2**), *N*-(2-aminoethyl)-3-aminopropyltrimethoxysilane (**3**) and *N*-(6-aminohexyl)-3-aminopropyltrimethoxysilane (**4**) (Scheme 3). CO_2 reacted with **1** and **2** with formation of bis-silylated organosilica precursors containing carbamate ammonium salts in the core while the reaction with **3** and **4** gave rise to a supramolecular network of silylated ammonium carbamate salts. The hydrolytic polycondensation of the ammonium carbamate precursors by the sol–gel process in an organic solvent provided the hybrid materials containing ammonium carbamate salts. Materials with well-defined lamellar structure containing ammonium carbamate salts were obtained from the carbamate prepared from **2** and **4**. Subsequent elimination of CO_2 upon heating generated materials with free amino groups in which the long-range order was maintained.

The structuration was found to be highly dependent on van der Waals interactions between the long alkylene chains.

(7) Alauzun, J.; Mehdi, A.; Reyé, C.; Corriu, R. J. P. *J. Am. Chem. Soc.* **2005**, *127*, 11205.
(8) (a) Hicks, J. C.; Dabestani, R.; Buchanan, A. C., III; Jones, C. W. *Chem. Mater.* **2006**, *18*, 5022. (b) Wang, X.; Lin, K. S. K.; Chan, J. C. C.; Cheng, S. *J. Phys. Chem. B* **2005**, *109*, 1763. (c) Macquarrie, D. J.; Jackson, D. B. *Chem. Commun.* **1997**, 1781. (d) Utting, K. A.; Macquarrie, D. J. *New J. Chem.* **2000**, *24*, 591.
(9) (a) Chujo, T.; Gonda, Y.; Oumi, Y.; Sano, T.; Yoshitake, H. *J. Mater. Chem.* **2007**, *17*, 1372. (b) Yokoi, T.; Yoshitake, H.; Yamada, T.; Kubota, Y.; Tatsumi, T. *J. Mater. Chem.* **2006**, 16. (c) Walcarius, A.; Etienne, M; Bessiere, J. *Chem. Mater.* **2002**, *14*, 2757. (d) Dai, S.; Hagaman, E. W.; Lin, J. S. *Chem. Mater.* **2001**, *13*, 2537. (e) Dai, S.; Burleigh, M. C.; Shin, Y.; Morrow, C. C.; Barnes, C. E.; Xue, Z. *Angew. Chem., Int. Ed.* **1999**, *38*, 1235. (f) Burleigh, M. C.; Markowitz, M. A.; Spector, M. S.; Gaber, B. P. *Chem. Mater.* **2001**, *13*, 4760. (g) Burleigh, M. C.; Dai, S.; Hagaman, E. W.; Lin, J. S. *Chem. Mater.* **2001**, *13*, 2537. (h) Yokoi, T.; Yoshitake, H.; Tatsumi, T. *J. Mater. Chem.* **2004**, *14*, 951.
(10) (a) Xu, X.; Song, C.; Andresen, J. M.; Miller, B. G.; Scaroni, A. W. *Energy Fuels* **2002**, *16*, 1463. (b) Huang, H.; Yang, R. T.; Chinn, D.; Munson, C. L. *Ind. Eng. Chem. Res.* **2003**, *42*, 2427. (c) Chang, A. C. C.; Chuang, S. S. C.; Gray, M.; Soon, Y. *Energy Fuels* **2003**, *17*, 468. (d) Khatri, R. A.; Chuang, S. S. C.; Soong, Y.; Gray, M. *Ind. Eng. Chem. Res.* **2005**, *44*, 3702. (e) Zheng, F.; Tran, D. N.; Busche, B. J.; Fryxell, G. E.; Addleman, R. S.; Zemanian, T. S.; Aardahl, C. L. *Ind. Eng. Chem. Res.* **2005**, *44*, 3099. (f) Khatri, R. A.; Chuang, S. S. C.; Soong, Y.; Gray, M. *Energy Fuels* **2006**, *20*, 1514.
(11) Hoerr, C. W.; Harwood, H. J.; Ralston, A. W. *J. Org. Chem.* **1944**, *9*, 201.
(12) Rudkevich, D. M.; Xu, H. *Chem. Commun.* **2005**, 2651.
(13) Brousseau, L.; Aurentz, D.; Benesi, A.; Mallouk, T. *Anal. Chem.* **1997**, *69*, 668.
(14) Herman, P.; Murtaza, Z.; Lakowicz, J. R. *Anal. Biochem.* **1999**, *272*, 87.
(15) Hampe, E. M.; Rudkevich, D. M. *Chem. Commun.* **2002**, 1450.
(16) Bates, E. D.; Mayton, R. D.; Ntai, I.; Davis, J. H. *J. Am. Chem. Soc.* **2002**, *124*, 926.
(17) Xu, H.; Rudkevich, D. M. *Chem. Eur. J.* **2004**, *10*, 5432.
(18) McClain, M. D.; Loy, D. A.; Prabakar, S. *Mater. Res. Soc. Symp. Proc. (Better Ceram. Chem. VII: Org./Inorg. Hybrid Mater.)* **1996**, *435*, 277.
(19) Shaltout, R. M.; Loy, D. A.; McClain, M. D.; Prabakar, S.; Greaves, J.; Shea, K. J. *Polym. Prepr. (Am. Chem. Soc., Div. Polym. Chem.)* **2000**, *41*, 508.
(20) Loy, D. A.; Beach, J. V.; Baugher, B. M.; Assink, R. A.; Shea, K. J.; Tran, J.; Small, J. H. *Chem. Mater.* **1999**, *11*, 3333.
(21) Bass, J. D.; Katz, A. *Chem. Mater.* **2003**, *15*, 2757.

The accessibility of the amino groups was proved by some complexation reactions and chemical transformations.

Experimental Section

All reactions were carried out under argon by using standard high vacuum and Schlenk techniques. Solvents were dried and distilled just before use. The following chemicals were purchased from Aldrich and used as supplied: 11-bromoundecene, 3-aminopropyltrimethoxysilane, *N*-(2-aminoethyl)-3-aminopropyltrimethoxysilane, and *N*-(6-aminohexyl)-3-aminopropyltrimethoxysilane.

11-Bromoundecyltrimethoxysilane. To a mixture of 11-bromoundecene (5.0 g, 21.4 mmol) and trimethoxysilane (5.23 mL, 43.0 mmol) in a Schlenk flask under nitrogen was added the Karstedt catalyst (108 μL of a 1 M THF solution) with a syringe. The reaction mixture was warmed at 80 °C for a night and then distilled under vacuum to give 6.09 g of 11-bromoundecyltrimethoxysilane as a colorless liquid. Yield 80%. Bp 90 °C at 0.04 Torr. ^{1}H NMR (200 MHz, $CDCl_3$): δ 0.60 (2H, t, $^2J_{H\text{-}H}$ = 8 Hz), 1.17 (2H, td, $^2J_{H\text{-}H}$ = 6 and 8 Hz), 1.2–1.4 (14H, m), 1.81 (2H, tt, $^2J_{H\text{-}H}$ = 6 and 8 Hz), 3.36 (2H, t, $^2J_{H\text{-}H}$ = 8 Hz), 3.78 (9H, s). ^{13}C NMR (50 MHz, $CDCl_3$): δ 10.3, 28.8, 22.7–33.1, 32.2, 51.2, 54.8. ^{29}Si NMR (40 MHz, $CDCl_3$): δ −45.6. SM (FAB$^+$, NBA): m/z = 356 [M + H$^+$] (60%).

11-Trimethoxysilylundecylazide 2. A quantity of sodium azide (2.46 g, 37.8 mmol) was added to a solution of 11-bromoundecyltrimethoxysilane (5.32 g, 15.0 mmol) in acetonitrile (55 mL). The reaction mixture was refluxed for 48 h. Then, the solvent was removed in vacuo, and the crude product was taken again in pentane (50 mL) and filtered. The filtrate was concentrated, and the remaining liquid was distilled under vacuum to yield 4.23 g of 11-trimethoxysilylundecylazide as a colorless liquid. Yield: 89%. Bp 111 °C at 0.05 Torr. ^{1}H NMR (200 MHz, $CDCl_3$): δ 0.61 (2H, t, $^2J_{H\text{-}H}$ = 7 Hz), 1.17 (2H, tt, $^2J_{H\text{-}H}$ = 6 and 8 Hz), 1.2–1.4 (14H, m), 1.58 (2H, t, $^2J_{H\text{-}H}$ = 8 Hz), 3.34 (4H, t, $^2J_{H\text{-}H}$ = 8 Hz), 3.78 (9H, s). ^{13}C NMR (50 MHz, $CDCl_3$): δ, 10.2, 28.7, 22.7–33.1, 32.8, 34.2, 54.8. ^{29}Si NMR (40 MHz, $CDCl_3$): δ −45.6. SM (FAB+, NBA): m/z = 304 [M + H]$^+$ (57%).

11-Amino-undecyltrimethoxysilane (2). A 50 mg quantity of palladium on carbon was added to a solution of 11-trimethoxysilylundecylazide (951 mg, 3.0 mmol) in anhydrous methanol (40 mL) placed in an autoclave under an argon atmosphere. After purging the autoclave, a 2 Torr H_2 pressure was applied for 30 min. The reaction mixture was then filtered, and the solvent was removed under vacuum. The residue was distilled to yield 716 mg of a colorless oil. Yield: 89%. Bp 116 °C at 0.04 Torr. ^{1}H NMR (200 MHz, $CDCl_3$): δ 0.61 (2H, t, $^2J_{H\text{-}H}$ = 8 Hz), 1.2–1.4 (14H, m), 1.45 (2H, tt, $^2J_{H\text{-}H}$ = 7 and 8 Hz), 1.51 (2H, tt, $^2J_{H\text{-}H}$ = 6 and 8 Hz), 2.66 (2H, t, $^2J_{H\text{-}H}$ = 8 Hz), 3.80 (9H, s). ^{13}C NMR (50 MHz, $CDCl_3$): δ, 10.1, 29.4, 22.6−33.0, 33.7, 42.1, 55.2. ^{29}Si NMR (40 MHz, $CDCl_3$): δ −45.4. SM (FAB+, NBA): m/z = 334 [M+H]$^+$ (45%).

Bis(aminopropyltrimethoxysilyl)ammonium Carbamate (1^C). CO_2 was bubbled at room temperature through a pure compound **1** (5.01 g, 27.9 mmol) placed in a flask of 25 mL under an inert atmosphere. The reaction was slightly exothermic, and CO_2 bubbling was maintained until the temperature of the mixture returned to room temperature yielding 5.57 g of a viscous liquid. Yield: 95%. ^{1}H NMR (200 MHz, $CDCl_3$): δ 0.64 (4H, t, $^2J_{H\text{-}H}$ = 8 Hz), 1.60 (4H, tt, $^2J_{H\text{-}H}$ = 7 and 8 Hz), 2.73 (4H, t, $^2J_{H\text{-}H}$ = 7 Hz), 3.82 (18H, s). ^{13}C NMR (50 MHz, $CDCl_3$): δ 8.0, 25.5, 44.1, 51.8, 163.2. ^{29}Si NMR (40 MHz, $CDCl_3$): δ −45.31. SM (FAB+, NBA): m/z = 403 [M + H]$^+$ (18%).

Bis(aminoundecyltrimethoxysilyl)ammonium Carbamate (2^C). This material was prepared from **2** according to the same procedure used to prepare **1^C**. Yield: 88%. ^{1}H NMR (200 MHz, $CDCl_3$): δ 0.63 (4H, t, $^2J_{H\text{-}H}$ = 8 Hz), 1.40 (28H, m), 1.58 (4H, tt, $^2J_{H\text{-}H}$ = 7 and 8 Hz), 1.65 (4H, tt, $^2J_{H\text{-}H}$ = 6 and 8 Hz), 2.70 (4H, t, $^2J_{H\text{-}H}$ = 8 Hz), 3.82 (18H, s). ^{13}C NMR (50 MHz, $CDCl_3$): δ 8.6, 20.6–24.4, 26.3, 49.8, 50.7, 166.7. ^{29}Si NMR (40 MHz, $CDCl_3$): δ −42.6. SM (FAB+, NBA): m/z = 262 [HO(MeO)$_2$Si(CH$_2$)$_{11}$NH$_3$]$^+$ (10%).

Bis(aminopropylaminoethyltrimethoxysilyl)ammonium Carbamate (3^C). This material was prepared according to the same procedure used to prepare **1^C**. A hard, colorless physical gel was obtained. Yield: 88%. ^{1}H NMR (200 MHz, $CDCl_3$): δ 0.62 (4H, t, $^2J_{H\text{-}H}$ = 7 Hz), 1.57 (4H, tt, $^2J_{H\text{-}H}$ = 7 and 8 Hz), 2.72 (4H, m), 3.52 (18H, s). ^{13}C NMR (50 MHz, $CDCl_3$): δ 22.8, 40.4, 49.5, 50.51, 52.1, 163.8. ^{29}Si NMR (40 MHz, $CDCl_3$): δ −42.00. SM (FAB+, NBA): m/z = 266 [(MeO)$_3$Si(CH$_2$)$_3$NCO$_2$(CH$_2$)$_2$NH$_3$ + H]$^+$ (8%). Anal. Calcd for $C_8H_{19}N_2O_5Si$: C, 38.2; N, 11.2; Si, 11.2. Found: C, 36.78; N, 11.12; Si, 10.82 (%).

Bis(aminopropylaminohexyltrimethoxysilyl)ammonium Carbamate (4^C). This material was prepared according to the same procedure used to prepare **1^C**. A hard, colorless physical gel was obtained. Yield: 90%. ^{1}H NMR (200 MHz, $CDCl_3$): δ 0.66 (4H, t, $^2J_{H\text{-}H}$ = 7 Hz), 1.50 (20H, m), 2.68 (12H, m), 3.57 (18H, s). ^{13}C NMR (50 MHz, $CDCl_3$): δ 7.0, 20.6, 22.1, 23.3, 49.2, 51.2, 52.4, 163.6. ^{29}Si NMR (40 MHz, $CDCl_3$): δ −41.21. SM (FAB+, NBA): m/z = 323 [(MeO)$_3$Si(CH$_2$)$_3$NCO$_2$(CH$_2$)$_6$NH$_3$ + H]$^+$ (20%).

Materials Syntheses. *General Procedure for Materials Containing Carbamate Ammonium Salts.* All the materials containing carbamate ammonium salts were prepared according to the same procedure. The preparation of **X1^C** is given as an example: **1^C** (2.01 g, 5.0 mmol) and pentane (5.0 mL) were introduced into a Schlenk tube. The suspension was stirred for 30 min in a thermostatted bath at 30 °C. Three molar equivalents of H_2O at pH = 1.5 were added (15 mmol, 270 μL of a 0.07 mol % HCl solution). Stirring was maintained for 4 h at 30 °C. Gelation took 12 h. The material was aged for 24 h at 30 °C, and the resulting solid was washed successively with 25 mL of acetone, 25 mL of ethanol, and 25 mL of ether and then was pulverized. That was done three times. The xerogel was dried for 1 h under vacuum (0.1 Torr) at 25 °C. A 1.18 g quantity of a white powder was obtained. Yield: 90%. ^{13}C cross-polarization magic-angle spinning (CP-MAS) NMR (75 MHz): δ 11.4, 23.7, 43.3, 164.7. ^{29}Si CP-MAS NMR (60 MHz): δ −59.71 (T^2, 8%), −68.03 (T^3, 92%). Anal. Calcd for $C_7H_{16}N_2O_5Si_2$: C, 31.8; N, 10.6; Si, 21.2. Found: C, 30.49; N, 9.61; Si, 20.80 (%).

X2^C. 2^C, 1.10 g (1.76 mmol); pentane, 1.76 mL; H_2O at pH 1.5, 95 μL of a 0.2 mol % HCl solution. Gelation time, 36 h; aging time, 48 h. Yield: 86% (0.74 g of a cream-white powder). ^{13}C CP-MAS NMR (75 MHz): δ 12.8, 22.2, 26.8, 29.4, 39.6, 48.8, 165.3. ^{29}Si CP-MAS NMR (60 MHz): δ −56.60 (T^2, 10%), −67.80 (T^3, 90%). Anal. Calcd for $C_{23}H_{48}N_2O_5Si_2$: C, 56.6; N, 5.7; Si, 11.5. Found: C, 54.80; N, 5.40; Si, 10.80 (%).

X3^C. 3^C, 1.10 g (2.25 mmol); pentane, 2.25 mL; H_2O at pH 1.5, 120 μL of a 0.2 mol % HCl solution. Gelation time, 48 h; aging time, 48 h. Yield: 88% (0.72 g of a pale yellow powder). ^{13}C CP-MAS NMR (75 MHz): δ 11.0, 19.2, 49.4, 54.4, 57.4, 164.3. ^{29}Si CP-MAS NMR (60 MHz): δ −58.50 (T^2, 5%), −66.00 (T^3, 95%). Anal. Calcd for $C_{12}H_{26}N_4O_7Si_2$: C, 36.52; H, 6.64; N, 14.24; Si, 14.20. Found: C, 37.81; H, 7.43; N, 14.22; Si, 14.41 (%).

X4^C. 4^C, 1.00 g (1.67 mmol); pentane, 1.67 mL; H_2O at pH 1.5, 90 μL of a 0.2 mol % HCl solution. Gelation time, 24 h; aging time, 24 h. Yield: 90% (0.69 g of a white powder). ^{13}C CP-MAS NMR (75 MHz): δ 12.8, 24.9, 29.3, 32.3, 43.2, 52.4, 55.0, 165.0. ^{29}Si NMR (60 MHz): δ −68.20 (T^3, 100%). Anal. Calcd for $C_{20}H_{42}N_4O_7Si_2$: C, 50.02; H, 8.00; N, 12.34; Si, 12.36. Found: C, 45.94; H, 8.81; N, 10.67; Si, 11.56 (%).

General Procedure for Materials Containing Free Amino Groups. All the materials containing carbamate ammonium salts were decarboxylated under 10^{-2} Torr at 80 °C for 12 h to give the corresponding materials containing free amino groups.

X1. A 500 mg quantity of $\mathbf{X1^C}$ released 38.1 mL of CO_2 (1.7 mmol) to yield the free amines containing material **X1** (95%) as a white powder. ^{13}C CP-MAS NMR (75 MHz): δ 11.4, 28.3, 45.8. ^{29}Si CP-MAS NMR (60 MHz): δ −58.97 (T^2, 5%), −67.91 (T^3, 95%). Anal. Calcd for $C_3H_8NO_{1.5}Si$: C, 32.7; N, 12.7; Si, 25.5. Found: C, 29.08; N, 10.44; Si, 24.50 (%).

X2. Yield: 92% as a white powder. ^{13}C CP-MAS NMR (75 MHz): δ 12.2, 23.6, 25.9, 30.3, 36.6, 45.8. ^{29}Si CP-MAS NMR (60 MHz): δ −58.50 (T^2, 10%), −66.90 (T^3, 90%). Anal. Calcd for $C_{11}H_{24}NO_{1.5}Si$: C, 59.5; N, 6.3; Si, 12.6. Found: C, 59.00; N, 6.10; Si, 11.90 (%).

X3. A 500 mg quantity of $\mathbf{X3^C}$ released 51.4 mL of CO_2 (2.3 mmol) to yield the free amines containing material **X3** (95%) as a white powder. ^{13}C CP-MAS NMR (75 MHz): δ 11.6, 24.3, 40.2, 53.6, 54.6. ^{29}Si CP-MAS NMR (60 MHz): δ −58.45 (T^2, 5%), −66.0 0 (T^3, 95%). Anal. Calcd for $C_5H_{10}N_2O_{1.5}Si$: C, 39.22; H, 8.56; N, 18.31; Si, 18.33. Found: C, 38.46; H, 8.38; N, 15.39; Si, 15.12 (%).

X4. A 500 mg quantity of $\mathbf{X4^C}$ released 41.2 mL of CO_2 (1.8 mmol) to yield the free amines containing material **X4** (95%) as a white powder. Yield: 95%. ^{13}C CP-MAS NMR (75 MHz): δ 12.8, 24.9, 29.3, 32.2, 35.3, 43.2, 52.4, 55.0. ^{29}Si CP-MAS NMR (60 MHz): δ −68.20 (T^3, 100%). Anal. Calcd for $C_9H_{21}N_2O_{1.5}Si$: C, 52.40; H, 8.70; N, 13.62; Si, 13.62. Found: C, 46.84; H, 9.08; N, 11.42; Si, 12.41 (%).

General Procedure for Complexation Reactions within the Materials **X1**, **X3**, *and* **X4.** All the complexation reactions were carried out according to the same procedure with standard high vacuum and dry argon techniques. The preparation of $\mathbf{X1^{CuCl_2}}$ is given as an example.

$\mathbf{X1^{CuCl_2}}$. A solution of $CuCl_2$ (3.67 g, 27.3 mmol, 1.5 equiv) in ethanol (15 mL) was added to 2 g (18.2 mmol) of **X1**. The resulting suspension was heated for 12 h under reflux with stirring. The solid was quantitatively recovered by filtration and washed with 25 mL of acetone, 25 mL of ethanol, and 25 mL of ether. After drying at 120 °C under vacuum, 3.16 g (98%) of $\mathbf{X1^{CuCl_2}}$ was obtained as a light green powder. The excess of copper salt contained in the reaction filtrate was titrated by conductimetry. Anal. Calcd for $C_6H_{16}N_2O_3CuCl_2Si_2$: C, 20.33; N, 7.94; Cu, 17.92; Cl, 20.01; Si, 15.81. Found: C, 23.11; N, 7.39; Cu, 15.95; Cl, 18.48; Si, 15.63 (%).

$\mathbf{X3^{CuCl_2}}$. 99% yield. Anal. Calcd for $C_5H_{13}N_2O_{1.5}CuCl_2Si$: C, 20.78; N, 9.71; Cu, 22.43; Cl, 24.73; Si, 9.72. Found: C, 20.80; N, 7.92; Cu, 21.45; Cl, 24.50; Si, 7.89 (%).

$\mathbf{X4^{CuCl_2}}$. 99% yield. Anal. Calcd for $C_9H_{21}N_2O_{1.5}CuCl_2Si$: C, 31.89; N, 8.34; Cu, 18.82; Cl, 20.91; Si, 8.30. Found: C, 30.05; N, 5.90; Cu, 15.01; Cl, 17.15; Si, 8.07 (%).

$\mathbf{X1^{Eu(NO_3)3}}$. 92% yield. Anal. Calcd for $C_9H_{24}N_6O_{13.5}EuSi_3$: C, 16.17; N, 12.56; Eu, 22.73; Si, 12.62. Found: C, 17.08; N, 10.66; Eu, 17.99; Si, 10.83 (%).

$\mathbf{X3^{EuCl_3}}$. 90% yield. Anal. Calcd for $C_5H_{13}N_2O_{1.5}EuCl_3Si$: C, 14.58; H, 3.25; N, 6.82; Eu, 36.91; Cl, 25.92; Si, 6.78. Found: C, 12.50; H, 3.75; N, 5.37; Eu, 32.31; Cl, 21.48; Si, 5.12 (%).

$\mathbf{X4^{Eu(NO_3)3}}$. 94% yield. Anal. Calcd for $C_{18}H_{42}N_9O_{12}EuSi_2$: C, 27.62; N, 16.13; Eu, 19.40; Si, 7.12. Found: C, 25.92; N, 10.83; Eu, 20.44; Si, 8.66 (%).

$\mathbf{X4^{Gd(NO_3)3}}$. 94% yield. Anal. Calcd for $C_{18}H_{42}N_9O_{12}GdSi_2$: C, 27.42; H, 5.28; N, 16.02; Gd, 27.42; Si, 7.11. Found: C, 24.94; H, 4.39; N, 11.03; Gd, 23.36; Si, 7.82 (%).

Depolymerization of **X1** *in Water.* In a 20 mL test tube, **X1** (2.2 g, 20.0 mmol) was added to demineralized water (7.8 g). The mixture was magnetically stirred. The complete solubilization of **X1** occurred within 45 min, giving rise to a perfectly transparent solution. ^{1}H NMR (200 MHz, D_2O): δ 0.41 (2H, m), 1.43 (2H, m), 2.52 (2H, m), 4.75 (3H, s). ^{13}C NMR (50 MHz, D_2O): δ 10.80, 24.32, 43.17. ^{29}Si NMR (40 MHz, D_2O): δ −40.2.

Chemical Transformations within **X1. X5**. Methyl acrylate (9.13 mmol, 0.79 g) was added to a suspension of **X1** (4.2 mmol, 1.11 g) in methanol (7 mL). The reaction mixture was stirred overnight at room temperature. The solid **X5** was recovered by filtration and washed successively three times with ethanol, acetone, and ether. The material **X5** was then dried at 90 °C under 0.1 Torr for 12 h to give 0.92 g (51%) of a cream colored powder. ^{13}C CP-MAS NMR (75 MHz): δ 11.15, 22.60, 33.83, 45.59, 49.70, 51.46, 172.93. ^{29}Si CP-MAS NMR (60 MHz): δ −67.20 (T^3, 100%). IR (KBr, cm^{-1}): 3435, 2949–2838, 1740, 1119–1033. Anal. Calcd for $C_7H_{14}NO_{3.5}Si$: C, 42.8; H, 7.14; N, 7.14; Si, 14.28. Found: C, 46.84; H, 9.08; N, 11.42.

X6. **X6** was prepared according to the same procedure used to prepare **X5** by reaction between **X1** (1.97 mmol, 0.52 g) and acrylic acid (3.94 mmol, 0.28 g) in ethanol (4 mL) to give 0.35 g (49%) of a cream colored powder. ^{13}C CP-MAS NMR (75 MHz): δ 10.94, 22.11, 32.87, 42.24, 49.03, 173.18. ^{29}Si CP-MAS NMR (60 MHz): δ −68.12 (T^3, 100%). IR (KBr, cm^{-1}): 3435, 2500, 2933, 2892, 2152, 1640, 1552, 1139, 1033. Anal. Calcd for $C_9H_{20}N_2O_5Si_2$: C, 36.99; H, 6.85; N, 9.56; Si, 19.18. Found: C, 40.15; H, 6.52; N, 8.17; Si, 19.97.

X7. **X7** was prepared according to the same procedure used to prepare **X5** by reaction between **X1** (2.54 mmol, 0.67 g) and glutaric anhydride (5.1 mmol, 0.51 g) in ethanol (16 mL) to give 0.58 g (54%) of a cream colored powder. ^{13}C CP-MAS NMR (75 MHz): δ 11.28, 23.52, 30.75, 43.15, 57.29, 174.64. ^{29}Si CP-MAS NMR (60 MHz): δ −66.92 (T^3, 100%). IR (KBr, cm^{-1}): 3309, 2933, 2884, 2552, 1727, 1634, 1552, 1131, 1021. Anal. Calcd for $C_9H_{20}N_2O_5Si_2$: C, 35.70; H, 6.25; N, 8.75; Si, 17.50. Found: C, 39.94; N, 9.97; Si, 17.84.

Materials Characterization. The ^{29}Si CP-MAS solid-state NMR spectra and ^{13}C CP-MAS solid-state NMR spectra were recorded on a BRUKER FTAM 300, in the latter case by using the TOSS technique. In both cases, the repetition time was 5 (for ^{13}C) and 10 s (for ^{29}Si) with contact times of 3 (for ^{13}C) and 5 (for ^{29}Si) ms. The duration of the ^{1}H pulse was 4.2 (for ^{13}C) and 4.5 (for ^{29}Si) μs, and the MAS rate was 10 (for ^{13}C) and 5 (for ^{29}Si) KHz. Chemical shifts (δ, ppm) were referenced to Me_4Si (^{13}C and ^{29}Si). The Fourier transform infrared spectra were obtained by using a Perkin-Elmer Series 2000 spectrometer. The preparation of the samples consisted of dispersing and gently grinding the powder in KBr.

Nitrogen adsorption isotherms were measured at −196 °C on a Micromeritics ASAP 2010 analyzer. The specific surface area of the samples was calculated using the Brunauer–Emmett–Teller (BET) method.

X-ray Diffraction (XRD) Spectroscopy. Powder XRD measurements were performed on an imaging plate 2D detector with a rotating copper anode apparatus (Cu Kα, λ = 1.542 Å) equipped with the focusing monochromator system OSMIC. Samples, which had been ground in an agate mortar under nitrogen, were placed in a glass Lindemann capillary tube of diameter 1 mm and length 80 mm. An acquisition time of 3000 s was used. The distance between the source and the detector was 180 mm, the plate diameter was 300 mm, and the beam size was 0.5 × 0.5 mm.

Conductimetric Titration. *Titration of Copper Salt.* The filtrate (obtained during the preparation of $\mathbf{X1^{CuCl_2}}$) was evaporated, and

Scheme 4

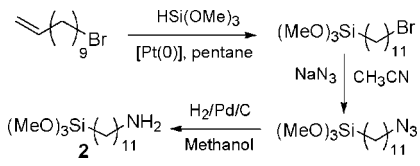

Scheme 5

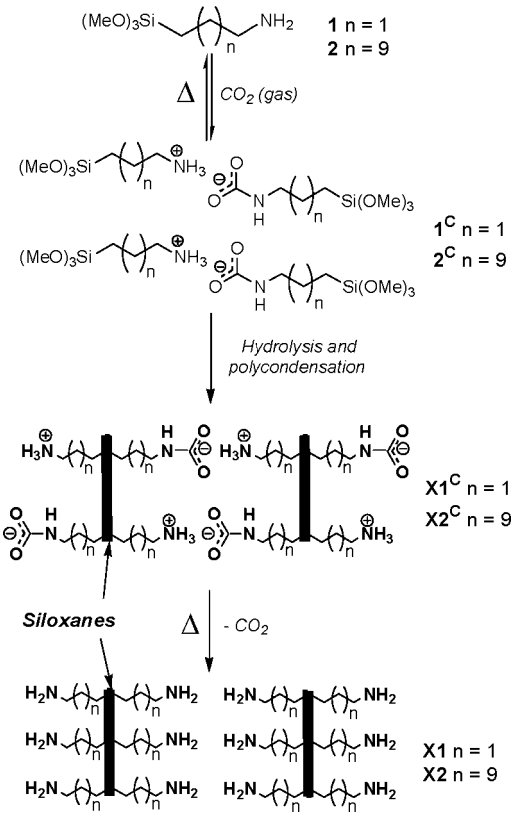

the residue was dissolved in deionized water (100 mL). A known volume of this solution (20 mL) was then titrated by an aqueous solution of cyclam (0.012 M). The conductance value was followed after each addition of cyclam. The inflection point of the titration curve was used to determine the exact amount of copper salt contained in the starting solution.

Elemental analyses were carried out by the "Service Central de Micro-Analyze du CNRS, Vernaison, France".

Results and Discussion

1.1. Synthesis of Hybrid Materials Containing Ammonium Carbamate Salts from the Primary Amines 1 and 2. **2** was prepared as depicted in Scheme 4: hydrosilylation of 11-bromoundecene gave rise to 11-bromoundecyltrimethoxysilane in 80% yield after distillation. The treatment of the 11-bromoundecyltrimethoxysilane with sodium azide afforded 11-trimethoxysilylundecylazide in 89% yield after distillation. Finally, the catalytic hydrogenation of the azide derivative provided **2** in 89% yield after distillation.

First, the reaction of CO_2 gas with the monosilylated primary amines **1** and **2** gave rise to bis-silylated alkylammonium alkylcarbamates $\mathbf{1^C}$ and $\mathbf{2^C}$, respectively, in high yield (Scheme 5, **C** is used to denote carbamates species).

To determine exactly the uptake of CO_2 per mole of **1** or **2**, the viscous liquids $\mathbf{1^C}$ and $\mathbf{2^C}$ were treated with a mixture

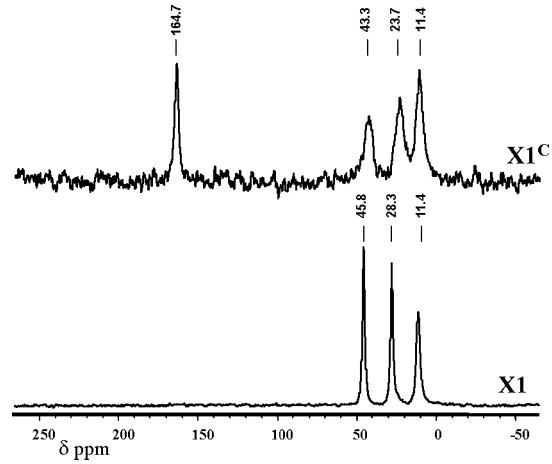

Figure 1. ^{13}C CP-MAS NMR spectra of $\mathbf{X1^C}$ (top) and **X1** (bottom).

of EtOH/H_2O at room temperature. The volume of CO_2 released was stored in a gas burette and measured very accurately; this indicated that the molar uptake of CO_2 per mole of precursor **1** and **2** was close to 0.5, which corresponds to the theoretical value for the CO_2 sequestration as an ammonium carbamate salt. Thus, the results of the titration indicated the quantitative formation of the carbamate salts from **1** and **2**, in accordance with Scheme 5. Compounds $\mathbf{1^C}$ and $\mathbf{2^C}$ were fully characterized by ^{1}H, ^{13}C, ^{29}Si NMR and mass spectroscopies. New resonances in the ^{13}C NMR spectra of $\mathbf{1^C}$ and $\mathbf{2^C}$at 163.2 and 166.7 ppm, respectively, attributed to the carbamate carbonyl carbon are particularly noteworthy.

As carbamates are not stable in water, the hydrolytic polycondensation of $\mathbf{1^C}$ and $\mathbf{2^C}$ was performed at 30 °C in the presence of a stochiometric amount of water at pH 1.5 in a 1 M pentane solution. Indeed, different organic solvents were first tried to achieve the sol–gel polymerization. While a slight release of CO_2 in ethanol and formamide was observed, the ammonium carbamates were perfectly stable in pentane. Gelation of $\mathbf{1^C}$ and $\mathbf{2^C}$ took 12 and 36 h, respectively, under these experimental conditions. After aging at 30 °C and work-up as described in the Experimental Section, xerogels, named $\mathbf{X1^C}$ and $\mathbf{X2^C}$, were obtained in high yield (**X** for xerogels and $\mathbf{1^C}$ and $\mathbf{2^C}$ to recall the precursors of the materials, Scheme 5).

The materials $\mathbf{X1^C}$ and $\mathbf{X2^C}$ were characterized by ^{13}C, ^{29}Si NMR spectroscopies and elemental analysis.

To prove that the ammonium carbamate salts remained intact during the sol–gel process, the volume of CO_2 released from the materials $\mathbf{X1^C}$ and $\mathbf{X2^C}$ was measured, as it was done from $\mathbf{1^C}$ and $\mathbf{2^C}$. In both cases, the expected values were obtained, indicating that the bridging groups did not decompose under these experimental conditions. The solid-state ^{13}C CP-MAS NMR spectra of $\mathbf{X1^C}$and $\mathbf{X2^C}$ displayed resonances at 164.7 and 165.3 ppm, respectively. They were attributed to the carbamate carbonyl carbon confirming the presence of the ammonium carbamate salts. Figure 1 shows the ^{13}C CP-MAS NMR spectrum of $\mathbf{X1^C}$. It exhibits three peaks at 11.4 ($SiCH_2$), 23.7 ($SiCH_2CH_2CH_2$), and 43.3 (NCH_2) in addition to the peak at 164.7 ppm.

The ^{29}Si CP-MAS NMR spectra of $\mathbf{X1^C}$ and $\mathbf{X2^C}$ revealed that both materials are well condensed. Indeed, the spectrum

Table 1. Composition of Materials X1^C, X2^C, X3^C, X4^C, X1, X2, X3, and X4 obtained from Elemental Analyses

sample	Si/C[a]	Si/N[a]
X1^C	0.29 (0.29)	1.08 (1.00)
X2^C	0.08 (0.09)	1.00 (1.00)
X1	0.36 (0.33)	1.07 (1.00)
X2	0.09 (0.09)	0.98 (1.00)
X3^C	0.16 (0.17)	0.51 (0.50)
X4^C	0.11 (0.10)	0.54 (0.50)
X3	0.18 (0.20)	0.49 (0.50)
X4	0.12 (0.11)	0.54 (0.50)

[a] In parentheses, theoretical values.

of **X1^C** exhibited resonances at −59.71 assigned to the T^2 substructure (8%) and at −68.03 ppm (T^3, 92%). This spectrum of **X2^C** displayed resonances at −56.60 (T^2, 10%) and −67.80 (T^3, 90%, see Supporting Information 1).

The Si/N and Si/C ratios for **X1^C** and **X2^C** determined by elemental analyses were found to be close to the theoretical values, showing thus that the organic groups remained intact (Table 1).

The powder XRD pattern for **X1^C** (see Supporting Information 2) exhibits a peak at $q = 4.55$ nm^{-1} accompanied by a second order reflection at $q = 7.66$ nm^{-1}. These peaks characterize a lamellar structure. The layer thickness (d) has been calculated from the low-angle peak using the Bragg law ($d = 2\pi/q$) and was found to be 1.38 nm. This observed d value is close to the theoretical distance between the two siloxane bridges (1.41 nm) obtained by a ChemDraw 3D calculation (Scheme 6A). The peak at $q =$ 15.7 nm^{-1} corresponds to 0.4 nm as the distance. This distance can be attributed to the alkylene chain packing within the layers.[22]

The XRD powder pattern for **X2^C** (Figure 2) exhibits four sharp diffraction peaks indicating a material with a long-range order. These peaks are clearly assigned to a lamellar structure. The interlayer distance d was found to be 3.21 nm. It is worth noting that this observed distance d is shorter than that calculated by the ChemDraw 3D length (3.54 nm) between the two siloxane bridges in the extended linear conformation (Scheme 6B). The peak at $q = 15.46$ nm^{-1} corresponding to 0.4 nm was also observed in the XRD pattern for **X1^C**. However, it appears less broad than for **X1^C** in accordance with a long-range order in this case.

The specific surface areas of both materials were found to be inferior to 10 m^2 g^{-1}.

1.2. Hybrid Materials Containing Free Primary Amino Groups. As our aim was to get materials with free amino groups, **X1^C** and **X2^C** were heated at 80 °C under 10^{-2} Torr for 12 h to remove the CO_2. The materials **X1** and **X2** were respectively obtained as white powders (**X1^C** and **X2^C** being prepared from **1** and **2**, respectively, Scheme 5).

It is very important to note the crucial role of CO_2 for obtaining materials. Under the same experimental conditions, the hydrolytic polycondensation of **1** or **2** instead of **1^C** or **2^C** did not afford any solid.

The solid-state ^{13}C CP-MAS NMR spectra of **X1** and **X2** show, in both cases, the absence of the peak attributed to the carbamate carbonyl carbon after thermal treatment of **X1^C** and **X2^C**. As an example, Figure 1 shows the ^{13}C CP-MAS NMR spectrum of **X1**. It exhibits three peaks at 11.4 (Si*C*H$_2$), 28.3 (SiCH$_2$CH$_2$*C*H$_2$), and 45.8 (N*C*H$_2$) showing that the propylene chain was maintained.

The ^{29}Si CP-MAS NMR spectrum of **X1** exhibited resonances at −58.97, assigned to the T^2 substructure (5%), and at −67.91 ppm (T^3, 95%) while the spectrum of **X2** displayed resonances at −58.50 (T^2, 50%) and −66.90 (T^3, 50%). These results show that the thermal decarboxylation involves a slight increase of the polycondensation degree.

The Si/N and Si/C ratios for **X1** and **X2** determined by elemental analyses were found to be rather close to the theoretical values, especially for **X2**, showing thus that the organic groups remained intact upon decarboxylation (Table 1).

The XRD powder pattern for **X1** displays only a diffraction peak at 5.19 nm^{-1} in addition to the peak at 15.7 nm^{-1}, indicating a short-range ordered structure (see Supporting Information 2). The d spacing of the first peak corresponds to 1.21 nm instead of 1.38 nm in **X1^C**. This distance fits well with the interlamellar distance between the two siloxane bridges after the release of CO_2. The absence of the second order in the XRD pattern of **X1**, while it was observed for the corresponding material **X1^C** containing carbamate salts, is to be noted; this should be due to the higher flexibility of the short alkylene chains in comparison to that of the bridged ammonium carbamate units in **X1^C**, which involves more disorder.

Interestingly, the XRD pattern for **X2** is exactly the same as that for **X2^C**, which indicates that the long-range order was perfectly maintained after the release of CO_2 without any shift of the long alkylene chains (Figure 2).

The specific surface areas of both materials were found to be inferior to 10 m^2 g^{-1}.

1.3. Synthesis of Hybrid Materials Containing Ammonium Carbamate Salts from the Diamines 3 and 4. CO_2 was bubbled at room temperature through the commercially available pure diamines **3** and **4**. The reaction was exothermic, and CO_2 bubbling was maintained until the temperature of the mixture returned to room temperature, affording the very viscous and translucent physical gels **3^C** and **4^C** (Scheme 7). The mass increase in both cases approached a molar uptake of CO_2 per mole of diamine **3** or **4**. The exact CO_2 uptake was also determined by measuring the volume of CO_2 released from a sample of **3^C** and **4^C** treated with a mixture of EtOH/H_2O at room temperature. These experiments confirmed that 1 equiv of CO_2 combines with 1 equiv of **3** or **4**, which corresponds to the theoretical value for the CO_2 sequestration involving both primary and secondary amino groups. The involvement of both amino groups, as expected, afforded a 2D supramolecular network of silylated ammonium carbamate salts represented in Scheme 7.

^{1}H, ^{13}C, ^{29}Si NMR and mass spectroscopies of gels **3^C** and **4^C** are in accordance with the structure of salts **3^C** and **4^C** proposed in Scheme 7. For instance, the resonances at 163.8 ppm for **3^C** and 163.6 ppm for **4^C** were attributed to

(22) Kaneko, Y.; Matsumoto, N. T.; Fujii, K.; Kurashima, K.; Fujita, T. *J. Mater. Chem.* **2003**, *13*, 2058.

Scheme 6. Calculated Interlayer Distances

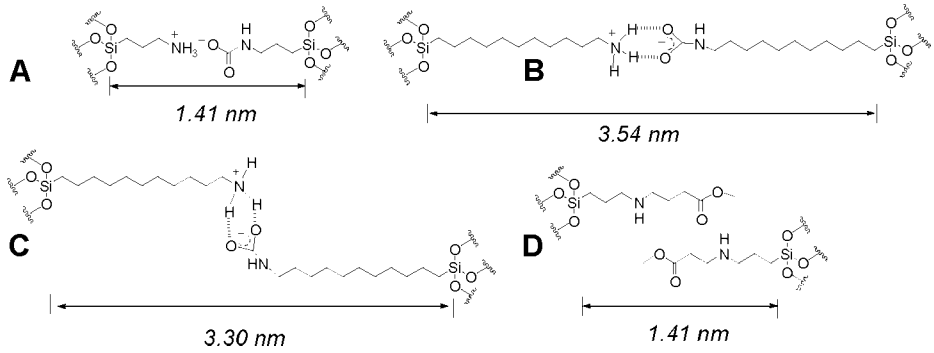

the carbamate carbon atom. The resonances at 52.1 and 49.2 ppm for $\mathbf{3}^{\mathbf{C}}$ and $\mathbf{4}^{\mathbf{C}}$, respectively, were assigned to the methylene groups attached to the carbamate nitrogen atom. It is also worth noting that only a signal was observed in the ^{29}Si NMR spectra of $\mathbf{3}^{\mathbf{C}}$ and $\mathbf{4}^{\mathbf{C}}$ (−42.00 ppm for $\mathbf{3}^{\mathbf{C}}$ and −41.21 ppm for $\mathbf{4}^{\mathbf{C}}$). These signals were attributed to the silicon atom of the $Si(OMe)_3$ groups, showing thus that the formation of physical gels occurred without any alteration of these hydrolyzable groups.

The hydrolytic polycondensation of $\mathbf{3}^{\mathbf{C}}$ and $\mathbf{4}^{\mathbf{C}}$ was achieved under the same conditions as for $\mathbf{1}^{\mathbf{C}}$ and $\mathbf{2}^{\mathbf{C}}$ (see the Experimental Section) affording the white powders $\mathbf{X3}^{\mathbf{C}}$ and $\mathbf{X4}^{\mathbf{C}}$, respectively.

The solid-state ^{13}C CP-MAS NMR spectra of $\mathbf{X3}^{\mathbf{C}}$ and $\mathbf{X4}^{\mathbf{C}}$ revealed that the supramolecular network of ammonium carbamate salts was maintained during the sol–gel process. That was mostly indicated by the resonances at 164.3 and 165.0 ppm for $\mathbf{X3}^{\mathbf{C}}$ and $\mathbf{X4}^{\mathbf{C}}$, respectively. The solid-state ^{13}C CP-MAS NMR spectra of $\mathbf{X4}^{\mathbf{C}}$ are reported in Figure 3.

The ^{29}Si CP-MAS NMR spectra of $\mathbf{X3}^{\mathbf{C}}$ and $\mathbf{X4}^{\mathbf{C}}$ (see Supporting Information 3) indicated that both materials are very well condensed. Indeed, the spectrum of $\mathbf{X3}^{\mathbf{C}}$ displayed a major resonance at −66.0 ppm, assigned to the T^3substructure, in addition to a very weak one (5%) at −58.5 ppm (T^2 substructure) while the spectrum of $\mathbf{X4}^{\mathbf{C}}$ exhibited only one signal at −68.2 ppm, assigned to the T^3 substructure.

The Si/N and Si/C ratios for $\mathbf{X3}^{\mathbf{C}}$ and $\mathbf{X4}^{\mathbf{C}}$ were inferred from the results of elemental analyses. They were found to be rather close to the theoretical values, showing thus that the organic groups remained intact (Table 1).

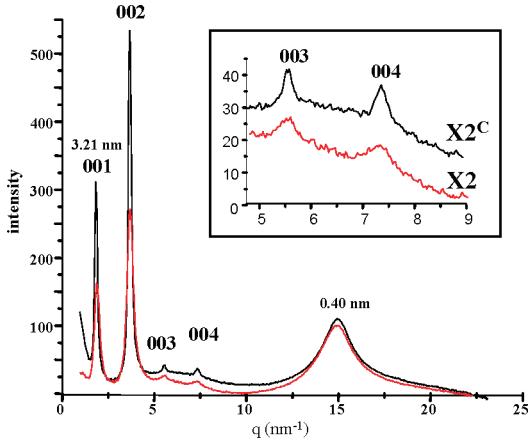

Figure 2. XRD patterns for $\mathbf{X2}^{\mathbf{C}}$ (black) and **X2** (red).

Scheme 7

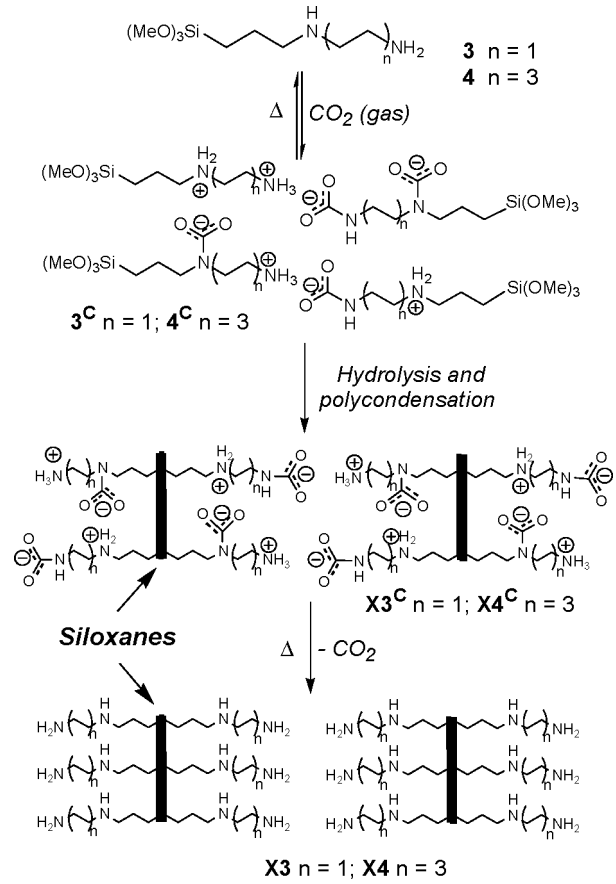

The XRD pattern of $\mathbf{X3}^{\mathbf{C}}$ (see Supporting Information 4) is rather similar to this of $\mathbf{X1}^{\mathbf{C}}$. Indeed, it exhibits an intense peak at $q = 3.80$ nm^{-1} corresponding to a distance of 1.63 nm. At higher angles, only the second order was observed at 7.15 nm^{-1} in addition to the broad peak at 0.42 nm attributed to alkylene chain packing within the layers.

The XRD pattern of $\mathbf{X4}^{\mathbf{C}}$ exhibits very sharp low-angle diffraction peaks (Figure 4). The first intense peak at $q =$ 2.00 nm^{-1} corresponds to the interlayer distance d, which was calculated to be 3.15 nm. At higher angles, the peaks observed at 1.54, 1.03, 0.78, and 0.62 nm are attributed to second, third, fourth, and fifth order diffractions, indicating a material with a well-ordered layered structure. Finally, the broad peak at 0.43 nm attributed to the alkylene chain packing within the layers was also observed.

It is worth noting that the interlayer distance obtained from the XRD pattern (3.15 nm) corresponds exactly to the length

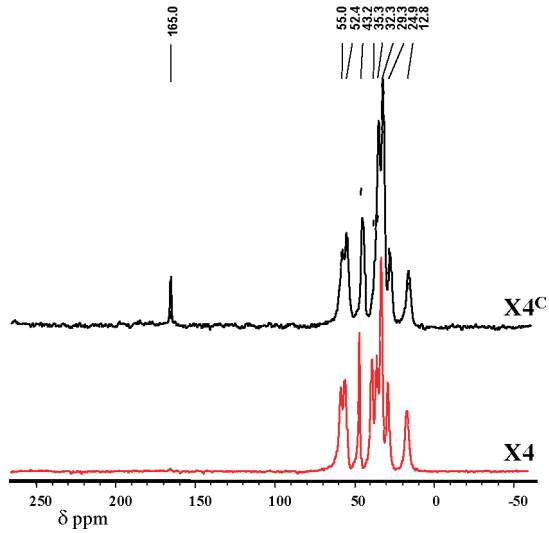

Figure 3. ^{13}C CP-MAS NMR spectra for **X4**^{C} (top) and **X4** (bottom).

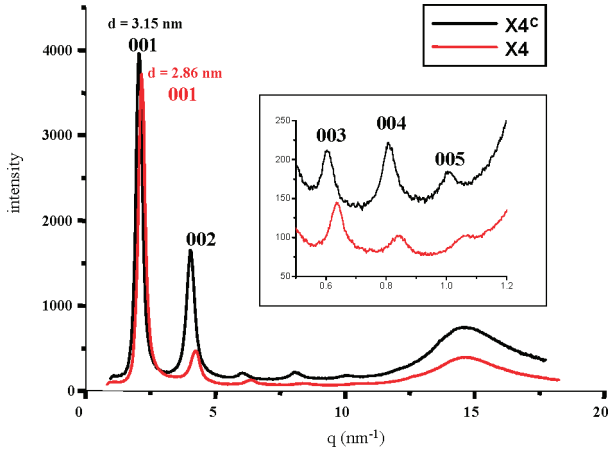

Figure 4. XRD patterns of **X4**^{C} (black) and of **X4** (red).

between the two siloxane bridges calculated by ChemDraw 3D in the extended linear conformation.

The specific surface areas of both materials were found to be inferior to 10 m^2 g^{-1}.

1.4. Hybrid Materials Containing Free Diamino Groups. To remove CO_2 and recover the amino groups, the materials **X3**^{C} and **X4**^{C} were heated at 80 °C under vacuum for 12 h, providing the materials **X3** and **X4**, respectively (**X3** and **X4** are used to recall the starting diamine derivatives **3** and **4**). The ^{13}C CP-MAS NMR spectra of **X3** and **X4** revealed in both cases the absence of the peak attributed to the carbamate carbonyl carbon after thermal treatment of **X3**^{C} and **X4**^{C}. The ^{13}C CP-MAS NMR spectra of **X4** was reported in Figure 3. It is worth noting that the peaks corresponding to the sp^3 carbon atoms of the alkylene chains are notably sharper than those observed in the corresponding materials **X3**^{C} and **X4**^{C}, which indicates a higher mobility of the chains. The ^{29}Si CP-MAS NMR spectra of **X3** and **X4** revealed that both materials are very well condensed, as were the materials **X3**^{C} and **X4**^{C}.

The Si/N and Si/C ratios for **X3** and **X4** were inferred from the results of elemental analyses. They were found to be rather close to the theoretical values (Table 1), showing thus that the decarboxylation did not affect the organic groups.

The XRD pattern of **X3** (see Supporting Information 4) exhibits only a peak, corresponding to a distance of 1.63 nm, in addition to the broad peak at 0.45 nm, indicating a low order of regularity for **X3**.

The XRD pattern of **X4** (Figure 4) exhibits a sharp and intense peak, corresponding to a distance of 2.86 nm, followed by peaks at higher angles (1.48, 0.99, 0.75, and 0.59 nm) attributed to the second, third, fourth, and fifth order characteristic of a well-ordered layered structure, respectively. It is worth noting that the five peaks were very slightly shifted in comparison to those of the corresponding material **X4**^{C}. This shift can be explained by the narrowing of the layers attributed to the decarboxylation.

Thus, upon decarboxylation, the long-range lamellar structure was maintained.

The specific surface areas of both materials were found to be inferior to 10 m^2 g^{-1}.

1.5. Self-Assembly Process and Study of XRD Patterns. We have shown that it is possible to obtain ordered materials containing amino and diamino functional groups starting from monosilylated amino derivatives **1**, **2**, **3**, and **4** by using CO_2 as an assembly agent. It is worth noting that the hydrolytic polycondensation of precursors **1**, **2**, **3**, and **4** does not afford materials under the same experimental conditions but gave rise to oligomers. Thus, the formation of the bis-silylated bridged derivatives **1**^{C} and **2**^{C} containing ammonium carbamate in the core as well as that of the supramolecular polysilylated networks **3**^{C} and **4**^{C} are required to obtain, in conclusion, ordered hybrid materials containing amino groups by the sol–gel process.

The formation of materials **X1**^{C}, **X2**^{C}, **X3**^{C}, and **X4**^{C} containing carbamate groups can be interpreted in the following way:

There is, first, hydrolysis of $Si(OMe)_3$ groups into silanol $Si(OH)_3$ while the alkylene chains of ammonium carbamate assemble. This assembly should involve the polycondensation of the silanol groups, which should be in close proximity. Starting from **2**^{C} and **4**^{C}, the sol–gel process involves the formation of a very well defined lamellar nanostructure while a less pronounced self-assembly resulted from the hydrolytic polycondensation of **1**^{C} and **3**^{C}. As the only difference between the bis-silylated precursors **1**^{C} and **2**^{C}, on one hand, and the supramolecular networks **3**^{C} and **4**^{C}, on the other hand, is the alkylene chain length, the better structuration observed for **X2**^{C} in comparison to that of **X1**^{C} and that of **X4**^{C} in comparison to that of **X3**^{C} should be due to the van der Waals interactions. These interactions should be strong enough in **X2**^{C} and **X4**^{C} to enforce an alignment of the alkylene chains, providing a well-defined lamellar structure. Thus, the long-range order was obtained during the sol–gel process. It does not precede it.

These results are in agreement with long-range order formed during the hydrolytic polycondensation in water of bridged organosilica with long alkylene chains [$(MeO)_3$-$Si(CH_2)_nSi(OMe)_3$ with $n = 12$ and 18].[5]

These interactions should be less strong in $\mathbf{X1^C}$and $\mathbf{X3^C}$ as the alkylene chains are shorter, which involves a less ordered assembly.

The layer thickness (*d*) in $\mathbf{X2^C}$ was found to be 3.21 nm, which is shorter than the length between the two siloxane bridges calculated by ChemDraw 3D in the extended linear conformation (3.54 nm, Scheme 6B). This result suggests that in $\mathbf{X2^C}$, the alkylene ammonium groups should be well aligned, on one hand, as well as the alkylenecarbamate groups, on the other hand, thanks to the van der Waals interactions. But both parts of the ammonium carbamate salts would be displaced as depicted in the Scheme 6C. In contrast, the layer thickness (*d*) in $\mathbf{X4^C}$ was found to be identical to the length between the two siloxane bridges calculated by ChemDraw 3D in the extended linear conformation. That suggests that, in this case, both parts of the ammonium carbamate salts should be aligned as depicted in Scheme 7.

Then, we have shown that the structural order observed in the materials $\mathbf{X1^C}$, $\mathbf{X2^C}$, $\mathbf{X3^C}$, and $\mathbf{X4^C}$ containing ammonium carbamate salts was maintained upon decarboxylation. Thus, the materials **X1** and **X3** present only a short-range order as $\mathbf{X1^C}$ and $\mathbf{X3^C}$, from which they originated, respectively. In both cases, there is a disappearance of the second order peak upon decarboxylation, which denotes more disorder in **X1** and **X3** than in $\mathbf{X1^C}$ and $\mathbf{X3^C}$. That should be due to the absence of the bridged ammonium carbamate units, which involves more flexibility.

In contrast, the materials **X2** and **X4** originating from $\mathbf{X2^C}$ and $\mathbf{X4^C}$, respectively, present a very well defined lamellar structure. It is remarkable to note that the XRD patterns for $\mathbf{X2^C}$ and **X2** are almost identical (Figure 2), revealing that the interlamellar distance did not change after the CO_2 release. We have previously noted that both parts of the carbamate salts should be displaced in $\mathbf{X2^C}$ (Scheme 6C). Upon CO_2 removal, as a consequence, NH_2 groups originating from both parts of the salt should be exactly facing each other, promoting hydrogen-bonding interactions. That could explain why the interlamellar distance is exactly the same in **X2** and $\mathbf{X2^C}$.

Both of the XRD patterns of **X4** and $\mathbf{X4^C}$ displayed five order peaks denoting materials with very well defined lamellar structure. It is worth noting that the five peaks were very slightly shifted in **X4** in comparison to those of the material $\mathbf{X4^C}$. Furthermore, in both cases, the interlamellar distance is very close to the distance calculated by Chemdraw 3D. This shift could be explained by the narrowing of the layers attributable to CO_2 removal.

2.1. Complexation of Copper and Lanthanide Salts within the Materials X1, X3, and X4. The accessibility of the amine functional groups in materials **X1**, **X3**, and **X4** as well as their chelating ability toward transition metal or lanthanide anhydrous salts was investigated. For that purpose, the materials were treated with an ethanolic solution of $CuCl_2$, $Eu(NO_3)_3$, or $Gd(NO_3)_3$. After heating under reflux arbitrarily for 12 h, the resulting solids were filtered off and copiously washed with ethanol to eliminate the noncomplexed salts. The filtrate containing the excess of salts was titrated by conductimetry for Cu^{2+} and complexometry measurements for lanthanide salts. The results obtained by titration were confirmed by elemental analyses of the materials after complexation (Table 2). The N/M molar ratio can give information about the ability of amino groups to act as ligands resulting from their distribution.

Table 2. Loading in Transition Metal or Lanthanide Ions Introduced per Gram of the Materials X1, X3, and X4

sample	salt	N/M[a] molar ratio	[metal][a] or [lanthanide][a] (mmol g^{-1})	[metal][b] or [lanthanide][c] (mmol g^{-1})
X1	$CuCl_2$	2.10	5.32	5.60
X3	$CuCl_2$	1.67	6.30	6.50
X4	$CuCl_2$	1.79	4.36	4.80
X1	$Eu(NO_3)_3$	6.44	2.75	3.03
X3	$EuCl_3$	1.81	6.25	6.52
X4	$Eu(NO_3)_3$	4.79	2.37	2.39
X4	$Gd(NO_3)_3$	4.68	2.56	2.40

[a] Calculated from elemental analysis. [b] Calculated from conductimetry titration. [c] Calculated from complexometry measurement.

The N/Cu molar ratio was found to be 2.10, 1.67, and 1.79 for **X1**, **X3**, and **X4**, respectively. That means that two amino groups are necessary on average for chelating one Cu^{2+} within **X1** and less than a diamine moiety within **X3** and **X4**, which is very low. Indeed, in solution, the complexation of Cu^{2+} requires generally four nitrogen atoms.[23] Thus, it appears that all the amino groups are operative as ligands and that in this case, long-range order does not improve considerably the chelating properties of the materials.

In the case of the complexation of europium salts, the N/Eu molar ratio was found to be 6.44, 1.81, and 4.79 for **X1**, **X3**, and **X4**, respectively. The N/Eu molar ratio within **X3** is particularly noteworthy when taking into account that the counterion is a chloride instead of a nitrate (Table 2). That means that the coordination number of the europium ions is probably unusually low as there is no possibility to extend the coordination number with either H_2O or SiOH groups. It is worth noting that a coordination number of six, which is low, was previously found for Eu^{3+} ions in ordered SBA-15 mesoporous silica containing chelating units.[24] In the present case, it appears that the diaminoethylene moieties are much more favorable for Eu^{3+} complexation than the diaminohexylene ones while the material **X3** containing diaminoethylene moieties is much less ordered than the material **X4** containing the diaminohexylene ones. Thus, as observed for copper complexation, the key point for the chelation of ions is the local distance between the amino groups and not the long-range order.

It is worth noting that complexation of $CuCl_2$ and $EuCl_3$ was also investigated within amine-free materials containing only long alkylene chains.[5] In all cases, a salt uptake inferior to 1% was obtained, showing thus that the salt uptake was due to a complexation reaction and not an adsorption within **X1**, **X3**, and **X4**.

2.2. Behavior of X1 in Water. We observed that the material **X1** presents an unusual behavior: it becomes entirely soluble when put into water at room temperature, giving rise to a transparent solution. The ^1H, ^{13}C, ^{29}Si NMR spectra of

(23) Dai, S.; Burleigh, M.; Shin, Y.; Morrow, C. C.; Barnes, C. E.; Xue, Z. *Angew. Chem., Int. Ed* **1999**, *38*, 1235.
(24) Corriu, R. J. P.; Mehdi, A.; Reyé, C.; Thieuleux, C.; Frenkel, A.; Gibaud, A. *New J. Chem.* **2004**, *28*, 156.

Scheme 8

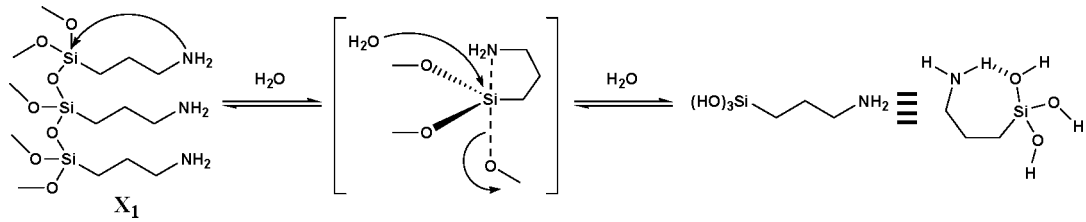

the resulting D_2O solution are in agreement with the formation of 3-aminopropyltrihydroxysilane (see the Experimental Section), which is stable in water. It is worth noting that while the ^{29}Si CP-MAS NMR spectrum of **X1** exhibited resonances at −58.97 (5%) and −67.91 ppm (95%), assigned to the T^2 and T^3 substructures, respectively, the ^{29}Si NMR spectrum of **X1** in the D_2O solution displayed only one signal at −40.2 ppm, characteristic of silanol. That indicates that there is no oligomer in aqueous solution.

Interestingly, it is possible to recover **X1** by simple removal of water. Several cycles (five) of polymerization−depolymerization for **X1** were established without any modification of the ^{29}Si NMR spectra, −40.2 ppm for the silanetriol and −58.97 ppm in addition to −67.91 ppm for **X1**, showing thus that the process is entirely reversible.

The depolymerization process can be explained by the formation of a pentacoordinate intermediate at the silicon resulting from the nucleophilic attack of the amino group (Scheme 8). This is a well-known process in silicon chemistry.[25] The coordination of the amino group to the silicon atom is very favorable in this case because of the formation of a five-membered ring. The pentacoordination at the silicon involves the lengthening of the Si−O−Si bonds, which become thus easily hydrolyzable in aqueous solution. That explains the fast depolymerization reaction of **X1** in water. Furthermore, the 3-aminopropyltrihydroxysilane is stabilized by intramolecular hydrogen bonding as depicted in Scheme 8, which explains the absence of oligomers in water.

2.3. Chemical Transformations within X1. As the material **X1** was easily prepared from **1**, it seemed to us of importance to prevent the depolymerization of **X1** in water. For that purpose, we attempted to transform the amino groups within **X1** into other functional groups also able to have chelating properties. An alcohol solution containing 1 equiv of methyl acrylate, acrylic acid, or succinic anhydride per amino group was added to the material **X1**. After stirring overnight at room temperature, the solids were copiously washed with ethanol, as described in the Experimental Section, affording the materials **X5**, **X6**, and **X7**, respectively (Scheme 9).

First of all, it is worth noting that no methyl acrylate was recovered in ethanol, which suggested that the chemical reaction was complete. In contrast, half the content in acrylic acid as well as in succinic anhydride was recovered in ethanol after the reaction. That suggests that an acid–base reaction giving rise to an ammonium carboxylate salt occurred within the solid.

(25) Chuit, C.; Corriu, R. J. P.; Reyé, C.; Young, J. C. *Chem. Rev.* **1993**, *93*, 1371.

Scheme 9

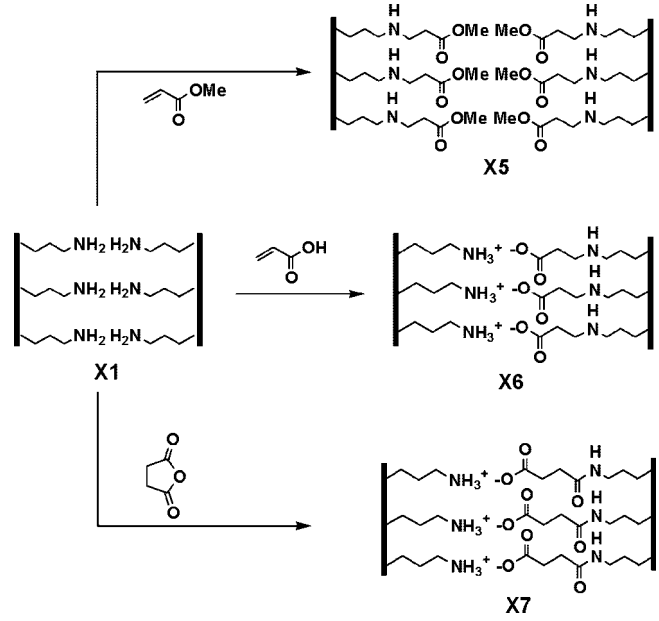

The materials were analyzed by IR spectroscopy. The Fourier transform (FT)-IR spectrum of **X5** displayed the typical absorption band at 1740 cm^{-1}attributed to the stretching vibration of the C═O groups of the ester functional group.

The formation of the ammonium carboxylate salts (Scheme 9) within **X6** was revealed by the FT-IR spectrum, which exhibited an intense band at 1640 cm^{-1} attributed to the stretching vibration of the C−O bonds of the carboxylate groups, the N−H stretching bands at 3435–2500 cm^{-1}, and the NH_3^+ bending band at 2151 cm^{-1}. Another NH bending band appeared at 1552 cm^{-1} in agreement with the secondary amino groups (Figure 5).

The FT-IR spectrum of **X7** also displayed the bands characterizing the formation of ammonium carboxylate salts (see the Experimental Section) in addition to the typical bands of the amides: 1634 cm^{-1} (νC═O of amide I), 1552

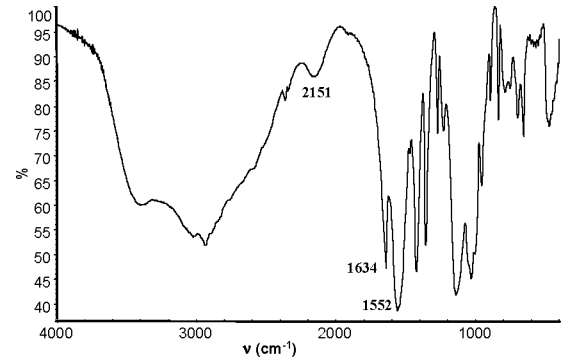

Figure 5. FT-IR spectrum of **X6**.

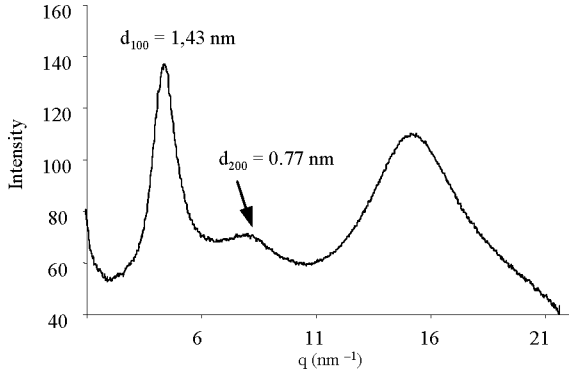

Figure 6. XRD pattern of **X5**.

cm^{-1} (δN−H of amide II), and νN−H at 3309 cm^{-1}. An absorption band at 1727 cm^{-1} appeared also, which was attributed to the presence of some hydrogen bonded carboxylic acid groups (see Supporting Information 5).

The ^{13}C CP-MAS NMR spectra of the materials **X5**−**X7** confirmed the formation of the reactions within the material **X1** as depicted in Scheme 9. The ^{13}C CP-MAS NMR spectrum of **X5** displays seven resonances as expected (see the Experimental Section), the more prominent one being the resonance at 172.93 ppm attributed to the carbonyl of the ester group. The ^{13}C CP-MAS NMR spectrum of **X6** exhibits six resonances, the most relevant signals being at 49.03 ppm, the signal attributed to carbons of the $^{+}NH_3CH_2$ moiety, and the signal at 173.18 ppm attributed to the carbon of the carboxylate groups. The ^{13}C CP-MAS NMR spectrum of **X7** exhibits a broad resonance at 174.64 ppm attributed to the carbons originating from both the amido groups and the carboxylate one.

The ^{29}Si CP-MAS NMR spectra of all the materials **X5**−**X7** displayed one resonance attributed to the T^3 substructures, which implies that the number of SiOH groups is negligible in the solids.

Elemental analysis of the resulting materials revealed that all the amino groups were accessible.

The XRD patterns of the materials **X5** and **X6** are very similar. Both of them revealed a slightly better structuration than in **X1**. The XRD pattern of **X5** is given as an example in Figure 6. It exhibits a 001 reflection at 1.43 nm, corresponding to the interlayer spacing, accompanied by a second order reflection at 0.77 nm characterizing a lamellar structure. These results indicate that not only did the intercalation of methyl acrylate and acrylic acid occur regularly but that it reinforced the structuration of the "host material". In such a way, the lamellar structure, which was present in $\mathbf{X1}^{C}$, appeared again. However, it is worth noting that the observed *d* value (1.43 nm) is very different from the distance between the two siloxane bridges obtained by ChemDraw 3D calculation in the extended linear conformation (2.41 for **X5** and 1.67 nm for **X6**). This difference between the obtained *d* value and the calculated one can be explained by the overlapping of the organic groups as depicted in Scheme 6D.

The XRD pattern of **X7** indicates two broad and badly defined reflections. This pattern suggests that the intercalation of the succinic anhydride occurred much less regularly than for the other two reagents, probably because of the steric hindrance of the molecule. As it was revealed from the FT-IR spectrum of **X7**, there is mostly a reaction between the two neighbor amino groups giving rise to ammonium carboxylate salts but also the formation of carboxylic acid groups, probably linked by hydrogen bonding with the amino groups. The presence of both reactions could explain the formation of a material with a lamellar structure not as regular as that of **X5** or **X6** that resulted from only one reaction.

These results show that the material **X1** containing the propyl amino groups is a sufficiently flexible system to allow the functionalization of the amino groups. However, a regular intercalation of organic groups seems to be possible only for small molecules. If there is some steric hindrance because of the size of the reagent, the intercalation will be also possible but not in a regular manner.

Conclusion

We have described a new approach to obtain ordered and amine-functionalized silica by using the reversible covalent binding of CO_2 to amines. The uptake of CO_2 on primary amines **1** and **2** gave rise to bis-silylated organosilica precursors containing ammonium carbamate salts in the core. CO_2 reacted with the diamines **3** and **4** to afford supramolecular networks of silylated ammonium carbamate. We found that the experimental conditions allow the hydrolytic polycondensation of these precursors without the decomposition of the carbamates. Hybrid materials with long-range order (lamellar structure) were obtained starting from **2** and **4**. The structuration occurred during the sol–gel process and was maintained upon CO_2 release. We evidenced that long-range order was promoted by van der Waals interactions between the long alkylene chains. Furthermore, we proved that these materials are able to chelate very high contents in transition metal or lanthanide ions; the content of ions depended on the local order and not on the long-range order. That renders these materials as good candidates for ion separation, including actinides. Finally, chemical transformations within the hybrid material containing propyl amino groups was possible. However, regular intercalation occurs only if the molecules that are introduced are rather small.

Supporting Information Available: CP-MAS NMR spectra, XRD patterns, and FT-IR spectra (PDF). This material is available free of charge via the Internet at http://pubs.acs.org.

CM701946W